

SYNTHESIS OF SBA-15 TYPE ORGANOSILICA SORBENTS USING SODIUM METASILICATE AND PHOSPHONIC ACID RESIDUES

Oksana Dudarko *, Yuriy Zub

Chuiko Institute of Surface Chemistry NAS of Ukraine, 17, General Naumov str., Kyiv 03164, Ukraine
*e-mail: odudarko80@gmail.com; phone: (+380) 444 229 630; (+380) 444 243 564

Abstract. The direct template method was used for the synthesis of mesoporous organosilica sorbents of SBA-15 type with phosphonic acid groups using sodium metasilicate (SS) as a source of silica. The presence of functional groups in the synthesized samples was confirmed by IR spectroscopy and elemental analysis. It was demonstrated that the increasing concentration of phosphorous-containing groups influenced the morphology and the spatial order of the porous structure of the samples. However, ordered mesoporous conglomerates can be identified in the resulting materials even when the content of functionalized phosphorus-containing silane in the reaction mixture is 33%. This approach allowed producing relatively cheap materials with ordered structure, developed specific surface (550-700 m²/g) and high sorption volume (0.74-0.81 cm³/g). The optimal sodium metasilicate (SS):diphosphoethyltriethoxysilane (DPTS) ratio for the synthesis of SBA-15 type organosilicas with phosphonic acid residues was found to be 10:2.

Keywords: SBA-15, phosphonic group, organosilica, characterization.

Received: 05 May 2017/ Revised final: 07 November 2017/ Accepted: 13 November 2017

Introduction

Adsorption is one of the most effective methods for water purification. Although water treatment technologies mostly use active carbons or synthetic sorbents, their use has a number of disadvantages, such as inefficient regeneration and problematic disposal. Therefore, the search for the new, cheap, effective and renewable sorbents is an urgent task. In this connection, organosilica sorbents, especially of SBA-15 type, are of great interest. They have a sufficiently stable structure, high efficiency, and selectivity, which can vary due to various factors, such as the nature of the functional layer, the concentration of the active groups, their affinity towards the adsorbing metals, sorption capacity, regeneration, etc. [1-5].

Alkoxysilanes of Si(OR)₄ structure, or bis-alkoxysilanes, which are most commonly used in the synthesis of such materials, are too expensive to be used in mass production. The usage of sodium metasilicate results in process cost reduction and the structural characteristics of the synthesized sorbents are not inferior to their expensive analogues. The development of new methods using sodium metasilicate (SS) as a source of silica started in 2000. Also, there are only a few works devoted to the factors

influencing mesoporous structure for functionalized silica [6-12] that can be regarded as a prerequisite for the development of cheap and promising SS based functionalized materials [13-15]. The most used sorbents are materials containing phosphonic acid groups, -P(O)(OH)₂ that form stable four- or six-membered complexes with rare earth ions, in various oxidation states. Therefore, phosphorus containing materials of inorganic and organic nature can be used as complexing sorbents [16-18] and are among the most extensively studied nowadays. The choice of such groups was based on sorption studies [19-23], as well as on previously obtained results [24,25].

This work presents the results of template synthesis of mesoporous organosilica from cheap sodium metasilicate under acidic conditions. To include P-containing functional groups, diethylphosphatoethyltriethoxysilane (DPTS) was chosen, since its hydrolysis in an acidic medium leads to the formation of P-containing oligomers and for comparison with our previous results, where we have used weak acidic conditions [14]. In order to study the DPTS influence on porosity and mesostructural ordering, its amount was varied during the synthesis process.

Experimental

Chemicals

Sodium metasilicate, $\text{Na}_2\text{SiO}_3 \cdot 9\text{H}_2\text{O}$ (SS, $\geq 98\%$ Aldrich, USA); diethylphosphatoethyl triethoxysilane, $(\text{C}_2\text{H}_5\text{O})_3\text{Si}(\text{CH}_2)_2\text{P}(\text{O})(\text{OC}_2\text{H}_5)_2$ (DPTS, 95%, Gelest, USA); poly(ethylene oxide)-poly(propylene oxide)-poly(ethylene oxide) Pluronic P123 block copolymer, $(\text{EO}_{20}\text{RO}_{70}\text{EO}_{20})$, 99%, BASF, USA); HCl; ethanol (absolute) were used as received in the synthesis of P-containing mesoporous silica.

Synthesis of phosphorus-containing mesoporous samples

The technique is based on the well-known method of template synthesis [26] with microwave treatment. Following the procedure for the Na-M [13], a series of samples was synthesized: **N1** (SS:DPTS=10:1); **N2** (SS:DPTS=10:2), **N3** (SS:DPTS=10:3); **N4** (SS:DPTS=10:5). The template was removed from mesophases with acidified ethanol in two stages for 12 hrs.

Measurements

The small angle XRD patterns were recorded over a range of $0.50 < 2\theta / ^\circ < 2.5$ on a PANanalytical. Inc. X'Pert Pro (MPD) Multi Purpose Diffractometer with $\text{CuK}\alpha$ radiation (0.154 nm) using an operating voltage of 40 kV and 40 mA, 20 s step time and 0.01 step size. Microscope glass slides were used as sample supports.

Transmission (TEM) and scanning electron microscopies (SEM) were used for structure and morphology investigations. The procedure of preparing samples for TEM involved their dispersion in ethanol (~5 wt.%). Following, each suspension was transferred to carbon/formvar-coated copper grids, dried under vacuum at 60°C for 3 hrs and examined using a JEM-1230 TEM (JEOL, Tokyo, Japan). SEM images were taken by JSM-6060 LV scanning electron microscope (JEOL, Japan).

Thermogravimetric (TG) analysis was performed on a TA Instruments TGA 2950 analyzer with $10^\circ\text{C min}^{-1}$ heating rate. Elemental analysis was performed by the Analytical Laboratory (the Institute of Organic Chemistry of NAS of Ukraine). IR reflectance spectra in the region of $4000\text{--}400\text{ cm}^{-1}$ were recorded on Thermo Nicolet Nexus FTIR spectrometer with diffuse reflection using the "SMART Collector" mode with a resolution of 8 cm^{-1} . Samples were mixed with KBr (Aldrich) at 1:20 ratio.

The textural properties of the synthesized samples were evaluated using the isotherms of nitrogen adsorption-desorption measured with

ASAP 2010 volumetric analyzer manufactured by Micrometrics, Inc. (Norcross, GA). Adsorption isotherms were measured at -196°C and the relative pressures ranging from 10^{-6} to 0.995 using ultra high purity nitrogen from Praxair Distribution Company (Danbury, CT, USA). Before analysis, the samples were degassed under vacuum for 2 hrs at 110°C until the residual pressure dropped to 6 or less μmHg . The Brunauer–Emmett–Teller (BET) [27] surface area (S_{BET}) was evaluated using adsorption data in the range of 0.05–0.2 p/p_0 , whereas the single-point total pore volume (V_{sp}) was estimated at 0.98 p/p_0 [28]. Pore size distributions and the maximum pore diameters (d_m) were determined by Kruk–Jaroniec–Sayari (KJS) method [29] based on the Barrett–Joyner–Halenda (BJH) algorithm [30].

The concentration of available phosphonic groups was determined by potentiometric titration. A batch of sample ($0.1 \pm 0.0005\text{ g}$) was mixed with 25 mL of 0.1 N NaNO_3 , equilibrated for 24 hrs, and titrated with 0.1 N NaOH solution, recording the pH values.

Results and discussion

The conditions for the synthesis of phosphorous-containing SBA-15 type sorbents based on sodium metasilicate (SS) have been determined previously [13]. The next step of our research was to investigate the effect of increasing the content of phosphorous-containing trialkoxysilane in the reaction mixture on the structural parameters of the sorbents. The activity and the availability of the functional layer are the key parameters of sorption. Thus, the main task of the study was to build as many sorption sites as possible, preserving the mesoporous SBA-15 type structure of the materials.

The comparative analysis of SEM images recorded for samples **N1**, **N2**, and **N3** (Figure 1) shows that at low mass fraction of DPTS (**N1**) the particles are more uniform in size and shape. The increase of DPTS content in the reaction mixture increases the polydispersity of the particles (**N2**) and even leads to the formation of particles of different shapes (**N3**). Thus, sample **N2** is mainly formed of particles close to spherical form with an approximate diameter of 50 to 500 nm. When the DPTS mass fraction exceeded 30% in the reaction mixture, the bulk of the sample consisted of irregular primary particles with areas of agglomerated sphere-like particles of ~ 520 nm in diameter. However, the primary particles were essentially fused with each other, without clear margins, neither between them, nor between their aggregates. A further increase of the mass fraction

of DPTS in the reaction mixture caused a decrease of the pH value. Under acidic conditions, hydrolysis occurred faster than condensation and therefore the resulting structure was weakly branched. The presence of P123 influences the kinetics of nucleation and growth of the primary particles of silica, tying the necessary water for the hydrolysis of the silanes. Furthermore, it is known that PEG reduces the dielectric constant of the solvent, promoting aggregation of primary particles.

TEM images confirm the presence of hexagonal structures (belonging to location of pores) indicating well-ordered derived synthesized materials (Figure 2). This pattern is typical for mesoporous materials SBA-15 type ($p6m$ symmetry group). The distances between pores centres for the samples N1, N2, and N3 were 7.8, 8.7, and 8.1 nm, respectively. Literature

sources indicate the difficulty of synthesis of well-ordered structures of SBA-15 type using a reaction mixture with a higher content of functionalized silane (greater than 20-25%) [31,32]. Earlier, we developed a synthetic approach [14], when individual ordered conglomerates were identified in the sample at 33% content of DPTS in the reaction solution. The modified synthesis technique used in the present study allows the preservation of SBA-15 type structure even at higher concentrations of functionalized silane due to performing the synthesis in more stringent conditions (differences in pH values of reaction mixtures). Another confirmation of this fact is that the structure of N3 was fairly ordered throughout all the bulk of the sample, not only in certain areas, as it was in the sample produced at the same alkoxy silanes ratio (DPTS content of 33%) [14].

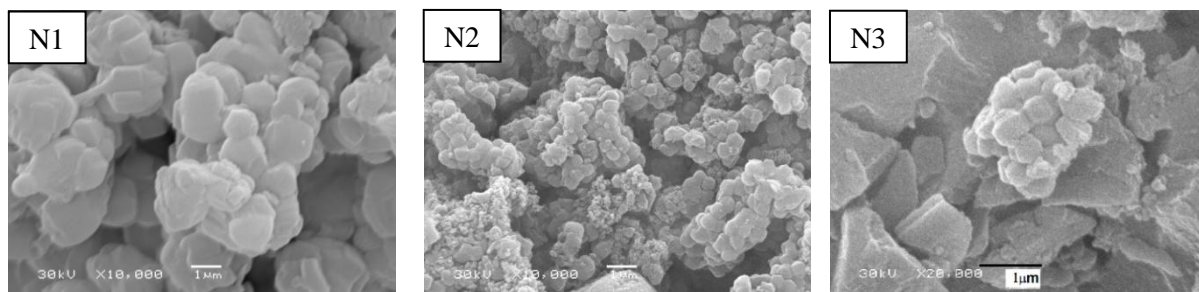


Figure 1. SEM images of synthesized samples.

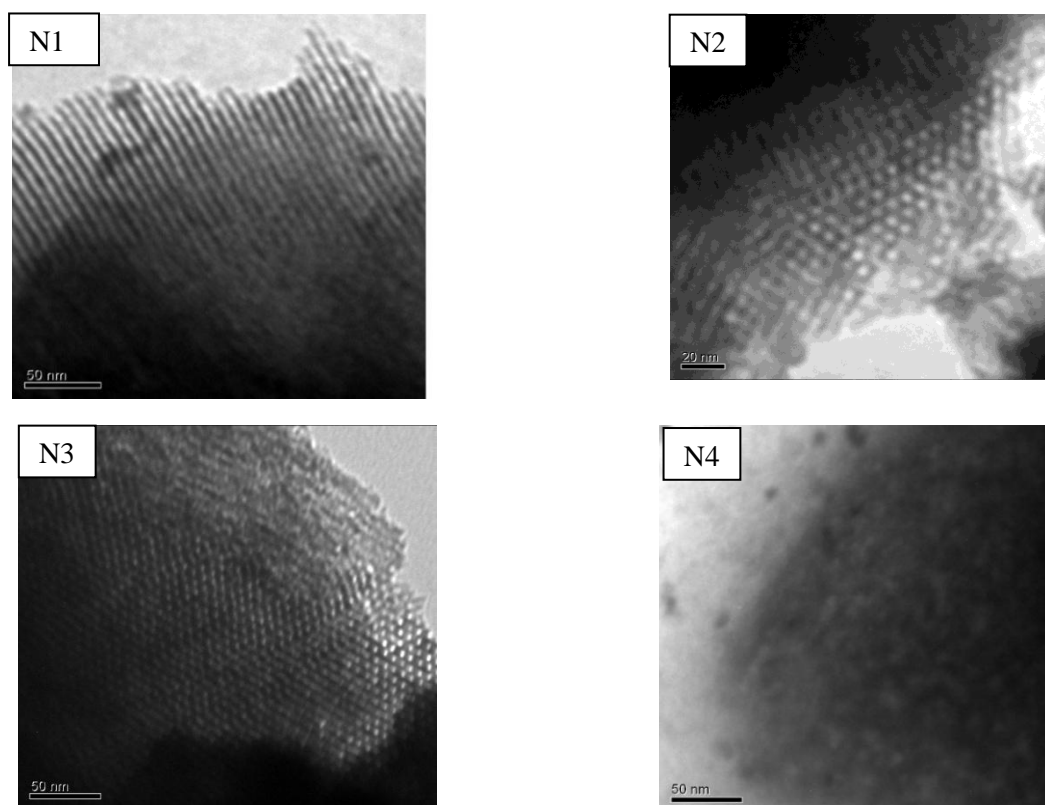


Figure 2. TEM images of the synthesized samples.

The next step was to investigate the influence of the SS:DPTS ratio on the stability of the sample structure using small-angle X-ray diffraction. XRD patterns of samples **N1** and **N2** contain three clearly defined peaks at 2θ (**N1**: 0.84° , 1.46° , 1.69° ; **N2**: 0.83° , 1.45° , 1.67° , see Figure 3). Samples **N3** and **N4** (Figure 3) have a less sharp peak at $2\theta \approx 0.86^\circ$ and 0.79° , respectively. The positions of these peaks

correspond to the 2D hexagonally ordered structures ($p6m$ group symmetry) and can be indexed as 100 (the highest XRD peak) and 110 and 200 (two less defined peaks). We assumed that at 10% mass fraction of DPTS in the solution the structure of the synthesized sample (**N1**) was close to the non-functionalized SBA-15. By increasing DPTS content up to 33% (**N3**), partial ordering remained in some areas.

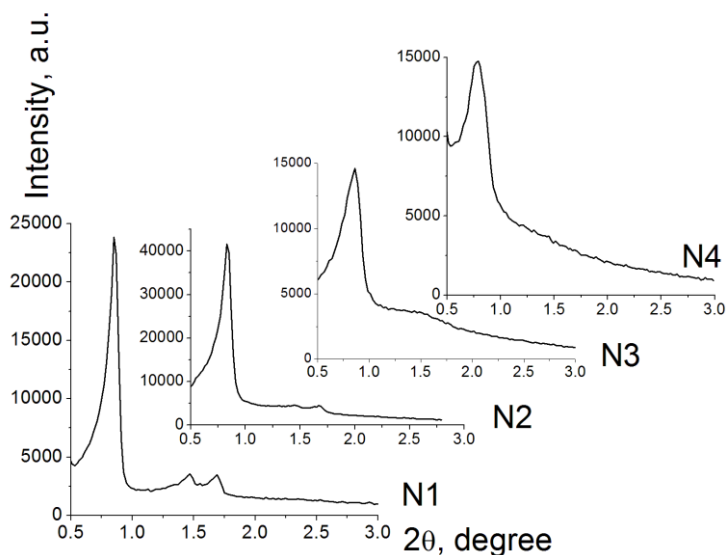


Figure 3. The XRD patterns of synthesized samples.

The IR spectra of the samples are typical for functionalized silica (see Figure 4). Thus, the IR spectra of both samples, **N1** and **N2**, registered the most intense band around $1000\text{--}1200\text{ cm}^{-1}$ with the shoulder in the high frequency region, assigned to $\nu_{\text{as}}(\text{SiOSi})$ vibrations. This indicates the presence of polysiloxane network [33]. The absorption band corresponding to the stretching vibrations of PO groups was identified around $\sim 1200\text{ cm}^{-1}$.

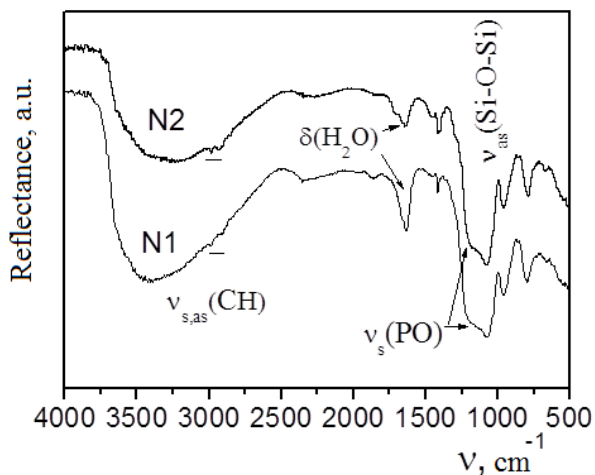


Figure 4. IR spectra of synthesized samples.

The absorption band of $-(\text{P}=\text{O})$ in the infrared spectrum of the DPTS was identified at 1241 cm^{-1} , while in the spectra of samples of phosphorous-containing silica it shifted by 40 cm^{-1} in the low frequency region and was registered as an intensive shoulder (Figure 4). In addition, the spectra are similar in the region of $1600\text{--}1657\text{ cm}^{-1}$ where they have low-intensity absorption bands corresponding to the deformation vibrations of water molecules. Above 3000 cm^{-1} there is a broad and intense absorption band due to the vibrations of OH groups from water molecules involved in the formation of hydrogen bonds. Thus, the IR spectra confirmed the presence of functional groups introduced on the surface layers of the synthesized materials.

Elemental analysis confirmed the presence of phosphorous in the samples **N1** and **N4** attributed to phosphonic groups with the concentration of 1.0 and 3.5 mmol/g, respectively [13].

Samples **N1** and **N4** presented the most notable differences in composition, therefore these were used for thermal analysis. According to the TGA, decomposition of the organic component of the synthesized materials started at

temperatures higher than 275°C (Figure 5). The residual extracting agent and physically adsorbed water were removed at temperatures up to 150°C. (The percentages of weight loss in this temperature range for **N1** and **N4** samples were 7% and 10%, respectively). The DTG curve of **N4** was very indicative in this respect. It is obvious that the amorphous structure prevents the complete removal of impurities from the pores and combustion occurs during several high intensity peaks, which show the steps of evaporation of the solvent and water, possibly from different layers of the sorbent. It should be mentioned that the DTG curve of sample **N4** features a peak around 500-600°C, which can be assigned to the destruction of the resulting oligomers. The weight loss in the temperature range (250-450°C) is in direct correlation with the content of introduced functional groups, this is clearly observed from DTG curves (9% for **N1**, 13% for **N4**). These weight losses represent additional evidence that the content of functional groups is proportional to the ratio of DPTS in the reaction mixture.

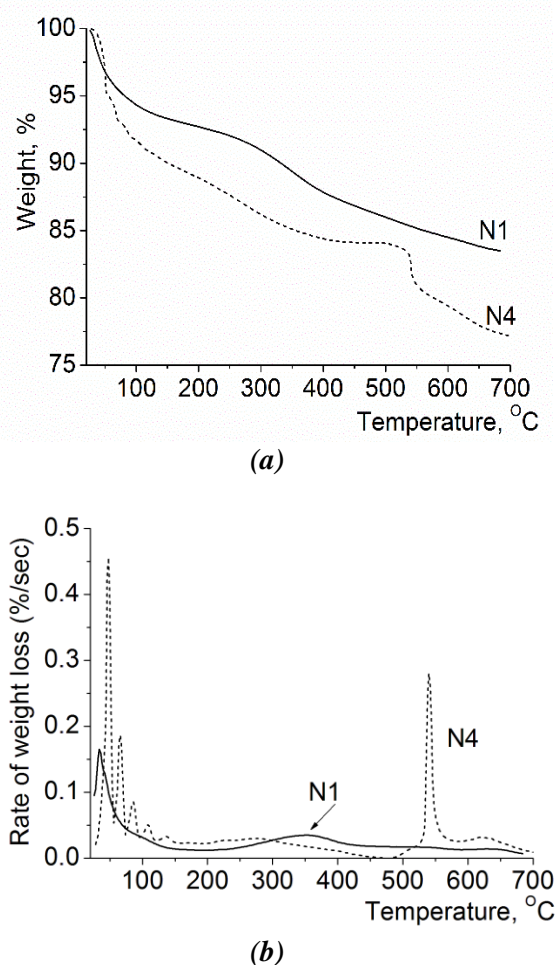


Figure 5. TGA (a) and DTG (b) curves of the synthesized samples.

Isotherms of nitrogen adsorption-desorption (measured at -196°C) and pore size distribution curves of samples **N1-N4** are shown in Figure 6. The isotherms are S-shaped and belong to Type IV according to the IUPAC classification (Figure 6(a)) [28]. Usually, for the sample with high content of functional groups, the adsorption curve is flatter, and the hysteresis loop has a lenticular shape, without the typical step for SBA-15. This indicates that the structure of the sample is less ordered. The specific surface area decreases from 700 to 550 m²/g in the range of samples **N1** → **N4** (Table 1). The isotherms of samples **N1** and **N2** are typical for the SBA-15 (Figure 6(a)). The pore-size distribution curves of these samples contain one clear narrow peak at 8.1 nm (**N1**) and 7.6 nm (**N2**) (Figure 6(b)), indicating the presence of uniform pores in the sample (see Table 1). Only the isotherm of **N1** (Figure 6(a)) has a clear hysteresis loop in the range of 0.6-0.8 p/p₀. This is typical for cylindrical mesopores with a narrow size distribution. The position and the size of the hysteresis loop depend on the content of the organic component. Thus, for the samples **N2** and **N3**, the hysteresis loop is shifted to the lower pressures and starts at 0.45 p/p₀, whereas for the sample **N4**, the lenticular-shaped hysteresis loop is stretched in a range of 0.45-0.85 p/p₀. The isotherm of the sample **N2** displays a special feature; it has a small step that indicates the existence of long pore constrictions/plugs. These results are in agreement with literature data for similar materials [34].

The pore size distribution curve of **N4** sample shows two peaks, so the sample has roughly the same amount of pores with effective diameters of 7.2 and 2.9 nm. Previously, we observed a similar feature for samples with high content of functional groups [14]. Although all samples had approximately the same wall thickness, this parameter was greater by 0.3 nm in sample **N4**, due to the higher content of functional groups in the surface layer.

The presence of functional groups on the surface was determined by potentiometric titration (Figure 7). The first peak of derivative for sample **N1** refers to the first stage: $\text{RH}_2\text{PO}_4 + \text{NaOH} \rightarrow \text{RNaHPO}_4 + \text{H}_2\text{O}$ (R - means $\equiv\text{Si}-(\text{CH}_2)_2-$), while the second is assigned to the next stage: $\text{RNaHPO}_4 + \text{NaOH} \rightarrow \text{RNa}_2\text{PO}_4 + \text{H}_2\text{O}$. It can be also concluded that the distribution of functional groups on the surface of sample **N3** (with higher concentrations of functional groups) is not uniform. As it was previously assumed [35-38], hydrogen bonds may form at a high density of

phosphonic groups on the surface that can cause multiple peaks on the differential potentiometric curve (Figure 7, sample **N3**), and can be explained by the gradual breaking of hydrogen bonds. The pK_1 values determined for samples **N1** (2.8)

and **N3** (3.4) suggest that the lower pK_1 value for **N1** corresponds to higher acidity of this sample, i.e. its groups dissociate and take part in the reactions more readily than of **N3** sample.

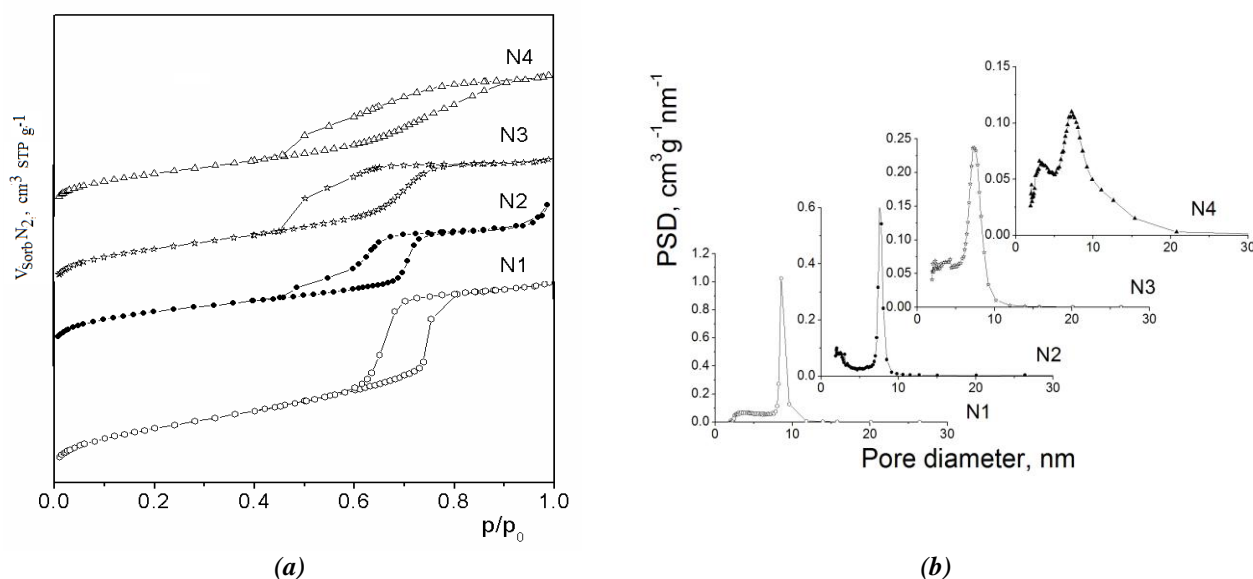


Figure 6. Isotherms of nitrogen adsorption-desorption (a) and the pore size distribution curves calculated by the KJS method (b)

Table 1

Parameters of the porous structure of the synthesized materials.						
Sample	Ratio SS:DPTS	S_{BET} , m^2/g	V_{sp} , cm^3/g	d_m^1 , nm	a_0^2 , nm	h_w^3 , nm
N1	10:1	700	0.77	8.1	11.9	2.0
N2	10:2	680	0.81	7.6	12.3	2.0
N3	10:3	630	0.74	7.4	11.6	2.0
N4	10:5	550	0.75	2.9, 7.2	13.2	2.3

¹pore diameter calculated using the KJS method;

²the distance between pore centres by TEM;

³pore wall thickness determined by XRD.

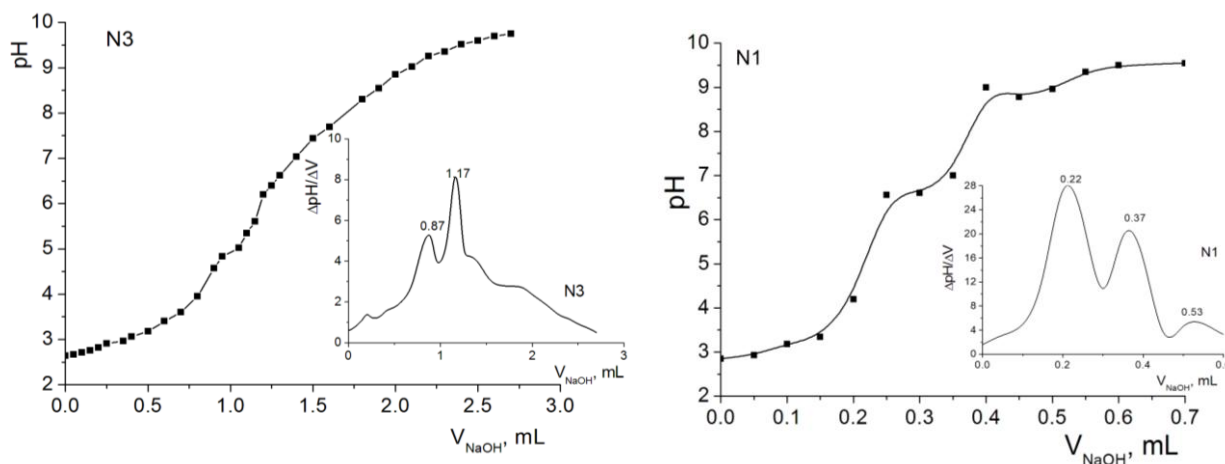


Figure 7. The potentiometric titration curves of the samples **N1** and **N3**, and their derivatives (the inserts).

Conclusions

We have developed a method of synthesis of phosphorous-containing organosilica materials of SBA-15 type. The key parameter that influences the structure forming processes is the ratio of the DPTS in the reaction mixture. The presence of functional groups on the surface layer was confirmed by IR spectroscopy, elemental analysis, and potentiometric titration. Increasing the mass fraction of DPTS (above 30%) leads to the formation of disordered structures. Therefore, the optimal SS:DPTS ratio for the synthesis of SBA-15 type organosilica sorbents with phosphonic acid residues is found to be 10:2. The resulting material is relatively cheap, has a well-ordered structure, developed specific surface ($680 \text{ m}^2/\text{g}$) and high sorption volume ($0.81 \text{ cm}^3/\text{g}$).

Acknowledgements

Authors express their gratitude to the Fulbright Scholar Program for the financial support of the current work (Grant ID 68120263, 2012-2013), and V.V. Sliesarenko for the help in development of the synthesis technique.

References

- Zhao, D.; Huo, Q.; Feng, J.; Chmelka, B.F.; Stucky, G.D. Nonionic triblock and star diblock copolymer and oligomeric surfactant syntheses of highly ordered, hydrothermally stable, mesoporous silica structures. *Journal of American Chemical Society*, 1998, 120(24), pp. 6024-6036. DOI: [10.1021/ja974025i](https://doi.org/10.1021/ja974025i).
- Colilla, M.; Balas, F.; Manzano, M.; Vallet-Regí, M. Novel method to enlarge the surface area of SBA-15. *Chemistry of Materials*, 2007, 19(13), pp. 3099-3101. DOI: [10.1021/cm071032p](https://doi.org/10.1021/cm071032p).
- Liu, M.; Hidajat, K.; Kawi, S.; Zhao, D.Y. A new class of hybrid mesoporous materials with functionalized organic monolayers for selective adsorption of heavy metal ions. *Chemical Communications*, 2000, 0(13) pp. 1145-1146. DOI: [10.1039/B002661L](https://doi.org/10.1039/B002661L).
- Hartmann, M.; Vinu, A. Mechanical stability and porosity analysis of large-pore SBA-15 mesoporous molecular sieves by mercury porosimetry and organics adsorption. *Langmuir*, 2002, 18(21), pp. 8010-8016. DOI: [10.1021/la025782j](https://doi.org/10.1021/la025782j).
- Liu, J.; Zhang, L.; Yang, Q.; Li, C. Structural control of mesoporous silicas with large nanopores in a mild buffer solution. *Microporous and Mesoporous Materials*, 2008, 116(1-3), pp. 330-338. DOI: <https://doi.org/10.1016/j.micromeso.2008.04.030>.
- Kim, J.M.; Stucky, G.D. Synthesis of highly ordered mesoporous silica materials using sodium silicate and amphiphilic block copolymers. *Chemical Communications*, 2000, 13, pp. 1159-1160. DOI: [http://dx.doi.org/10.1039/B002362K](https://doi.org/10.1039/B002362K).
- Choi, M.; Heo, W.; Kleitz, F.; Ryoo, R. Facile synthesis of high quality mesoporous SBA-15 with enhanced control of the porous network connectivity and wall thickness. *Chemical Communications*, 2003, 0(12), pp.1340-1341. DOI: <https://doi.org/10.1039/B303696K>.
- Kosuge, K.; Sato, T.; Kikukawa, N.; Takemori, M. Morphological control of rod- and fiberlike SBA-15 type mesoporous silica using water-soluble sodium silicate. *Chemistry of Materials*, 2004, 16(5), pp. 899-905. DOI: [10.1021/cm030622u](https://doi.org/10.1021/cm030622u).
- Fulvio, P.F.; Pikus, S.; Jaroniec, M. Short-time synthesis of SBA-15 using various silica sources. *Journal of Colloid and Interface Science*, 2005, 287(2), pp. 717-720. DOI: <https://doi.org/10.1016/j.jcis.2005.02.045>.
- Wang, W.; Shan, W.; Ru, H. Facile preparation and new formation mechanism of plugged SBA-15 silicas based on cheap sodium silicate. *Journal of Materials Chemistry*, 2011, 21(43), pp. 17433-17440. DOI: <https://doi.org/10.1039/C1JM13669K>.
- Ding, Y.; Yin, G.; Liao, X.; Huang, Z.; Chen, X.; Yao, Y. Key role of sodium silicate modulus in synthesis of mesoporous silica SBA-15 rods with controllable lengths and diameters. *Materials Letters*, 2012, 75, pp. 45-47. DOI: <https://doi.org/10.1016/j.matlet.2012.01.091>.
- Rahmat, N.; Hamzah, F.; Sahiron, N.; Mazlan, M.; Zahari, M.M. Sodium silicate as source of silica for synthesis of mesoporous SBA-15. *IOP Conference Series: Materials Science and Engineering*, 2016, 133, pp. 012011. DOI: <https://doi.org/10.1088/1757-899X/133/1/012011>.
- Dudarko, O.A.; Gunathilake, C.; Sliesarenko, V.V.; Zub, Y.L.; Jaroniec, M. Microwave-assisted and conventional hydrothermal synthesis of ordered mesoporous silicas with P-containing functionalities. *Colloids and Surfaces A: Physicochemical and Engineering Aspects*, 2014, 459, pp. 4-10. DOI: <https://doi.org/10.1016/j.colsurfa.2014.06.036>.
- Dudarko, O.A.; Gunathilake, C.; Wickramaratne, N.P.; Sliesarenko, V.V.; Zub, Y.L.; Górka, J.; Dai, S.; Jaroniec, M. Synthesis of mesoporous silica-tethered phosphonic acid sorbents for uranium species from aqueous solutions. *Colloids and Surfaces A: Physicochemical and Engineering Aspects*, 2015, 482, pp. 1-8. DOI: <https://doi.org/10.1016/j.colsurfa.2015.04.016>.
- Li, D.; Zhu, X. Short-period synthesis of high specific surface area silica from rice husk char. *Materials Letters*, 2011, 65(11), pp. 1528-1530. DOI: <https://doi.org/10.1016/j.matlet.2011.03.011>.
- Cholin, Y.; Zaitsev, V. The complexes on the surface of chemically modified silica. *Folio: Kharkov*, 1997, 136 p. (in Russian).

17. Lisichkin G.V. Ed. Chemistry of grafted surface compounds. Fizmatlit: Moscow, 2003, 592 p. (in Russian).
18. Sinyavskaya, E.I.; Tsymbal, L.V.; Bogatyrev, V.M. Obtaining and complexing properties of phosphoryl ligands grafted onto the silica surface. Adsorption and adsorbents, 1984, 12, pp. 51-55 (in Russian).
19. Lebed, P.J.; Souza, K.; Bilodeau, F.; Larivière, D.; Kleitz, F. Phosphonate-functionalized large pore 3-D cubic mesoporous (KIT-6) hybrid as highly efficient actinide extracting agent. Chemical Communications, 2011, 47(41), pp. 11525-11527. DOI: <https://doi.org/10.1039/c1cc14053a>.
20. Yuan, L.Y.; Liu, Y.L.; Shi, W.Q.; Lv, Y.-L.; Lan, J.-H.; Zhao Y.-L.; Chai Z.-F. High performance of phosphonate-functionalized mesoporous silica for U(VI) sorption from aqueous solution. Dalton Transactions, 2011, 40(28), pp. 7446-7453. DOI: <http://doi.org/10.1039/C1DT10085H>.
21. Wang, X.L.; Yuan, L.Y.; Wang, Y.F.; Li, Z.J.; Lan, J.H.; Liu, Y.L.; Feng, Y.X.; Zhao, L.Y.; Chai, Z.F.; Shi, W.Q. Mesoporous silica SBA-15 functionalized with phosphonate and amino groups for uranium uptake. Science China Chemistry, 2012, 55(9), pp. 1705-1711. DOI: <https://doi.org/10.1007/s11426-012-4625-7>.
22. Vertinskaya, T.E.; Fadeev, V.I.; Milchenko, D.V. Sorption of titanium (IV) and thorium (IV) by phosphonic acid silica-based sorbents. Journal of Analytical Chemistry, 1986, 41(6), pp. 1067-1071. (in Russian).
23. Cholin, Y.V.; Zaitsev, V.N.; Zaitsev, G.N.; Merniy, S.A. Complex formation in the adsorption layers of silica grafted with groups of aminophosphonic and aminodiphosphonic acids. Russian Journal of Inorganic Chemistry, 1995, 40(2) pp. 275-283. (in Russian).
24. Dudarko, O.A.; Goncharik, V.P.; Semeni, V.Ya.; Zub, Yu.L. Sorption of Hg^{2+} , Nd^{3+} , Dy^{3+} , and UO_2^{2+} ions at polysiloxane xerogels functionalized with phosphonic acid derivatives. Protection of Metals, 2008, 44(2), pp. 193-197. DOI: <https://doi.org/10.1134/S003317320802015X>.
25. Milyutin, V.V.; Gelis, V.M.; Nekrasova, N.A.; Melnyk, I.V.; Dudarko, O.A.; Sliarenko, V.V.; Zub Y.L. Sorption of actinide ions onto mesoporous phosphorus-containing silicas. Radiochemistry, 2014, 56(3), pp. 262-266. DOI: <https://doi.org/10.1134/S1066362214030072>.
26. Celer, E.B.; Jaroniec, M. Temperature-programmed microwave-assisted synthesis of SBA-15 ordered mesoporous silica. Journal of American Chemical Society, 2006; 128(44), pp. 14408-14414. DOI: <https://doi.org/10.1021/ja065345h>.
27. Brunauer, S.; Emmett, P.H.; Teller, E. Adsorption of gases in multimolecular layers. Journal of American Chemical Society, 1938, 60(2), pp. 309-319. DOI: [10.1021/ja01269a023](https://doi.org/10.1021/ja01269a023).
28. Thommes, M.; Kaneko, K.; Neimark, A.V.; Olivier, J.P.; Rodriguez-Reinoso, F.; Rouquerol, J.; Sing, K. S. W. Physisorption of gases, with special reference to the evaluation of surface area and pore size distribution (IUPAC Technical Report). Pure Applied Chemistry, 2015, 87(9-10), pp. 1051-1069. DOI: <https://doi.org/10.1515/pac-2014-1117>.
29. Jaroniec, M.; Solovyov, L.A. Improvement of the Kruk-Jaroniec-Sayari method for pore size analysis of ordered silicas with cylindrical mesopores. Langmuir, 2006, 22(16), pp. 6757-6760. DOI: [10.1021/la0609571](https://doi.org/10.1021/la0609571).
30. Barrett, E.P.; Joyner, L.G.; Halenda, P.P. The determination of pore volume and area distributions in porous substances. I. Computations from nitrogen isotherms. Journal of American Chemical Society, 1951, 73(1), pp. 373-380. DOI: [10.1021/ja01145a126](https://doi.org/10.1021/ja01145a126).
31. Sims, S.D.; Burkett, S.L.; Mann, S. Synthesis of hybrid inorganic-organic mesoporous silica by co-condensation of siloxane and organosiloxane precursors. Materials Research Society Symposium Proceedings, 1996, 431, pp. 77-82.
32. Burkett, S.L.; Sims, S.D.; Mann, S. Synthesis of hybrid inorganic-organic mesoporous silica by co-condensation of siloxane and organosiloxane precursors. Chemical Communications, 1996, 11, pp. 1367-1368. DOI: [10.1039/CC9960001367](https://doi.org/10.1039/CC9960001367).
33. Smith, A. Applied Infrared Spectroscopy. Wiley: New York, 1979, vol. 54, 336 p.
34. Saravanamurugan, S.; Sujandi, S.; Han, D.-S.; Koo, J.-B.; Park S.-E. Transesterification reactions over morphology controlled amino-functionalized SBA-15 catalysts. Catalysis Communications, 2008, 9(1) pp. 158-163. DOI: <https://doi.org/10.1016/j.catcom.2007.06.002>.
35. Dabrowski, A.; Barczak, M.; Dudarko, O.A.; Zub, Yu.L. Preparation and characterisation of polysiloxane xerogels having covalently attached phosphonic groups. Polish Journal of Chemistry, 2007, 81(4), pp. 475-483.
36. Gunathilake, C.; Kadanapitiye, M.S.; Dudarko, O.; Huang, S.D.; Jaroniec, M. Adsorption of lead ions from aqueous phase on mesoporous silica with P-containing pendant groups. ACS Applied Materials & Interfaces, 2015, 7 (41), pp. 23144-23152. DOI: [10.1021/acsami.5b06951](https://doi.org/10.1021/acsami.5b06951).
37. Aliev, A.; Ou, D.L.; Ormsby, B.; Sullivan, A.C. Porous silica and polysilsesquioxane with covalently linked phosphonates and phosphonic acids. Journal of Materials Chemistry, 2000, 10(12), pp. 2758-2764. DOI: [10.1039/B007452G](https://doi.org/10.1039/B007452G).
38. Bibent, N.; Charpentier, T.; Devautour-Vinot, S.; Mehdi, A.; Gaveau, P.; Henn, F.; Silly, G. Solid-state NMR spectroscopic studies of propylphosphonic acid functionalized SBA-15 mesoporous silica: characterization of hydrogen-bonding interactions. European Journal of Inorganic Chemistry, 2013, 13, pp. 2350-2361. DOI: [10.1002/ejic.201201404](https://doi.org/10.1002/ejic.201201404).